Journal of Hazardous Materials, 9 (1984) 315—346
Elsevier Science Publishers B V , Amsterdam — Printed in The Netherlands

INFLUENCE OF TURBULENCE ON GAS EXPLOSIONS*

BJØRN H HJERTAGER

Chr Michelsen Institute, Dept of Science and Technology, N 5036 Fantoft, Bergen (Norway)

(Received April 24, 1984, accepted June 29, 1984)

Summary

A description of the current status of knowledge on flame and pressure development in turbulent gas explosions is presented Special emphasis is given to gas explosions occurring in obstacle environments The problem is discussed in relation to experimental results obtained in both large-scale and small-scale situations, as well as results from theoretical studies Special attention is given to the influence of confinement, obstacle shape and distribution, mode of propagation (axial, radial and spherical), fuel—air mixture and scaling characteristics

1. Introduction

1 1 The problem

Production, transport and handling of large quantities of flammable gases has focused attention on the need to predict flame and pressure development in possible accidental explosions If reliable and realistic predictions of the consequences can be made, then the choice of realistic safety measures and/or optimum design strategy is improved Explosion propagation in integrated industrial systems is highly dependent on the geometric configuration This is due to the fact that the rate of heat release and mixing are dependent on turbulence parameters, and these parameters are again dependent on the flow inside the geometry It is well accepted that the most effective means of increasing turbulence and thus the violence of explosions is to place obstacles in the way of the flame propagation path Other turbulence-producing mechanisms like Rayleigh—Taylor instability and buoyancy have also been identified as increasing the violence of gas explosions However, these effects are of minor importance if obstacles are present in the explosion space

The influence of obstacles on flame and pressure development has been studied experimentally by various workers [1—6], and the qualitative models governing the acceleration mechanism are well established Quantitative

*Presented at the International Symposium on the Control and Prevention of Gas Explosions, London, December 1, 1983

0304-3894/84/$03 00

methods capable of modelling these processes are, however, scarce The present author [7, 8] has proposed and validated a method which seems to reproduce some of the experimental trends The basis of this method is to treat the intimate coupling between flow, turbulence, heat release, mixing and pressure rise by use of submodels for each of the elementary processes which are participating

1 2 Purpose of this paper

The present paper will review the status of knowledge in flame and pressure development in turbulent gas explosions Both experimental and theoretical results are discussed

2 Basic considerations

2 1 Obstacle acceleration

In an industrial plant located either on-shore or off-shore we may have the following hazard situation Flammable gases may be released due to a gasket failure, a pipe rupture or even a vessel rupture During and after the release, the flammable gas will entrain air and form an explosible gas cloud

In this situation we may have the explosible mixture within a rather untidy, semi-confined area If we then have an ignition source at some point, and the gas cloud begins to burn, the combustion products expand and push the unburnt gas ahead of the flame If there are obstacles in the path of the expansion, we get shear layers in the flowing unburnt gas because we have a velocity gradient which generates turbulence When the flame eventually reaches these turbulent regions, the rate of heat release increases We thus have a mechanism driven by the combustion which gives expansion The expansion in turn gives flow, the flow produces turbulence, and the turbulence enhances the combustion rate We therefore have an acceleration mechanism Of course, the ultimate result in a semi-confined geometry is that we have a pressure load Depending on various parameters this pressure load may attain a wide range of values ranging from a few millibars and up to full detonation pressure of the order of 20 bars It is therefore of prime importance to establish the relationships between the pressure load and the various parameters, like confinement, obstacle layout, fuel—air type and stoichiometry If such data are available from suitable prediction methods, the basis for adoption of realistic safety measures to minimize the consequences will be improved In order to develop such prediction methods experiments in relevant scale and geometry must be performed

2 2 Mode of flame propagation

When a flame propagates in a flammable mixture three classical types of modes may be identified, namely axial, cylindrical and spherical modes In the axial mode all gas expansion following combustion gives rise to increased velocity ahead of the flame, due to the constant flow area This situation

is relevant for rooms or volumes with large length-over-diameter ratios, L/D, and with openings only at either end In the cylindrical mode the combustion-generated velocity ahead of the flame may be smaller due to area increase along the propagation path, i e , the area is proportional to the distance from ignition This situation may be relevant for rooms or volumes bounded by two walls, top and bottom The spherical mode is characterized by an area increase along the flame path which is proportional to the distance-from-ignition squared, thus indicating a smaller velocity ahead of the glame than for both axial and cylindrical modes This situation is relevant for volumes with openings in all directions If the ignition source is a point source all explosions will start in the spherical mode and may be subsequently modified, depending on the internal obstacle layout and on the bounding walls of the confinement

3. Experimental studies

3 1 Influence of obstacles

The author and his colleagues have undertaken a fairly large research programme to investigate the influence of turbulence-producing obstacles on flame and pressure development in large-scale gas explosions The experimental facility used is schematically shown in Fig 1 Experiments using both methane—air and propane—air in obstructed tube geometries have been conducted

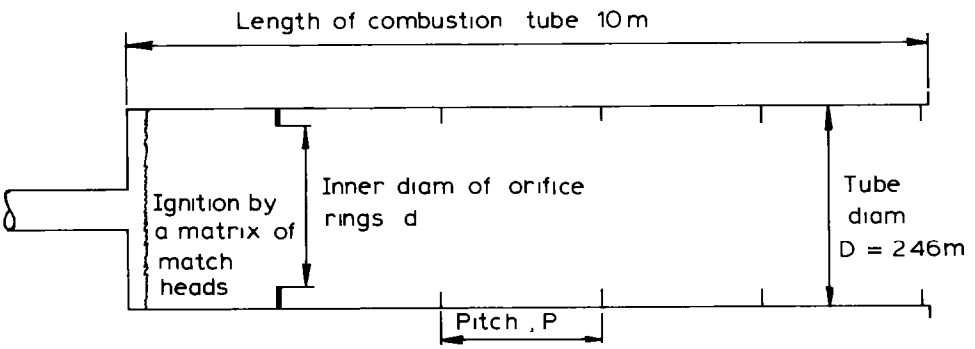

Fig 1 Schematic view of geometry for flame acceleration experiment (1) H (height of ring) = 0 1 m, d = 2 26 m, BR = 0 16, (2) H = 0 2 m, d = 2 06 m, BR = 0 3, (3) H = 0 37 m, d = 1 74 m, BR = 0 5

The observed influence of obstacles is perhaps best illustrated by comparing explosions with no obstacles to the most violent explosion observed With no obstacles and methane—air mixtures, the maximum overpressure observed in the tube was 0 12 bar and the outside air blast overpressure was 0 03 bar 10 m from the tube exit The most violent explosion was obtained with 6 orifice plates with a blockage ratio, BR, of 0.3 In this test the outside blast strength at 10 m was 0 46 bar and the maximum pressure in the

tube (8 86 bar) was larger than the theoretical closed vessel maximum overpressure (7.83 bar) Methane—air explosions in other obstacle configurations are characterized by overpressures between these two extremes Even with very small obstacles of BR = 0 16 and with only one obstacle of $BR \geqslant 0.5$, overpressures larger than 1 bar were observed in the vessel A summary of the methane—air data is shown in Fig 2 These data show that the effect of obstacles inside a vented vessel gives pressure loads which are higher and outside the commonly used venting codes

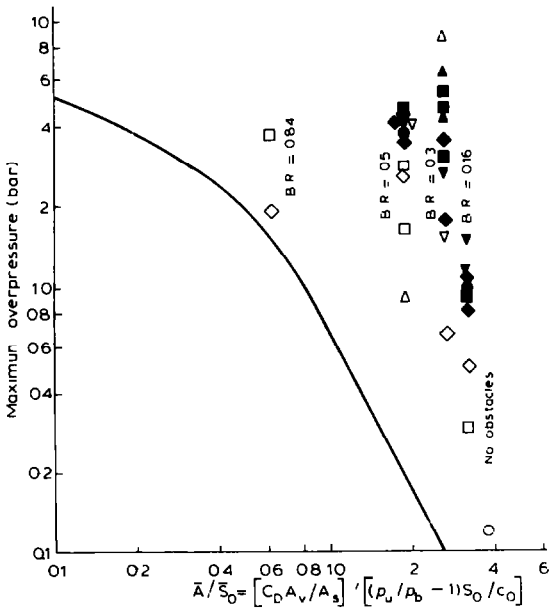

Fig 2 Comparison of present results with safe recommended vent areas for central ignition in near spherical vessels proposed by Bradley and Mitcheson ○ — No obstacles, ◇ — plate, x = 1 65 m, □ — 1 plate, x 5 13 m, △ — 1 plate, x = 9 3 m, ▽ — 2 plates, ◆ 3 plates, ● — 4 plates (p = 2 5 m), ■ — 5 plates (p = 2 m), ▲ — 6 plates (p = 1 5 m), ▽ — 9 plates (p = 1 m) (Moen et al [5])

Influence of fuel—air and stoichiometry

Having shown that methane—air mixtures produce larger pressures than previously anticipated, the question of the effects of turbulence on other fuel—air mixtures arises With regard to sensitivity to detonation methane is classified among the least hazardous fuels (Matsui and Lee [9]) However, fairly recently it has been shown that addition of even small quantities of higher alkanes to methane, such as for example propane, markedly increases the sensitivity to detonation (Bull et al [10]).

So far the possibility of a similar effect has been more or less ignored when considering combustion acceleration by turbulence, the reason being that the thermodynamic properties of various hydrocarbon—air mixtures

are roughly the same and that the laminar flame speed is almost identical for a number of alkane—air mixtures Studies of turbulent deflagration waves in hydrocarbon—air mixtures in the past have indicated also that the flame propagation is related only to the laminar flame speed and turbulence parameters, and not to the spontaneous ignition delay which is relevant for detonation sensitivity ranking

Hjertager et al [6] have studied the flame and pressure development of propane—air in the aforementioned tube geometry and they found that for the same geometrical conditions the violence of propane—air explosions was much stronger than that of the corresponding methane—air explosions reported by Moen et al [5] The most violent explosion was observed with 5 orifice plates and a blockage ratio of BR = 0 5 In this particular test the average maximum overpressure was 7 bar, the outside blast at 10 m was 0 61 bar and the maximum peak overpressure at the tube exit was 13 9 bar The

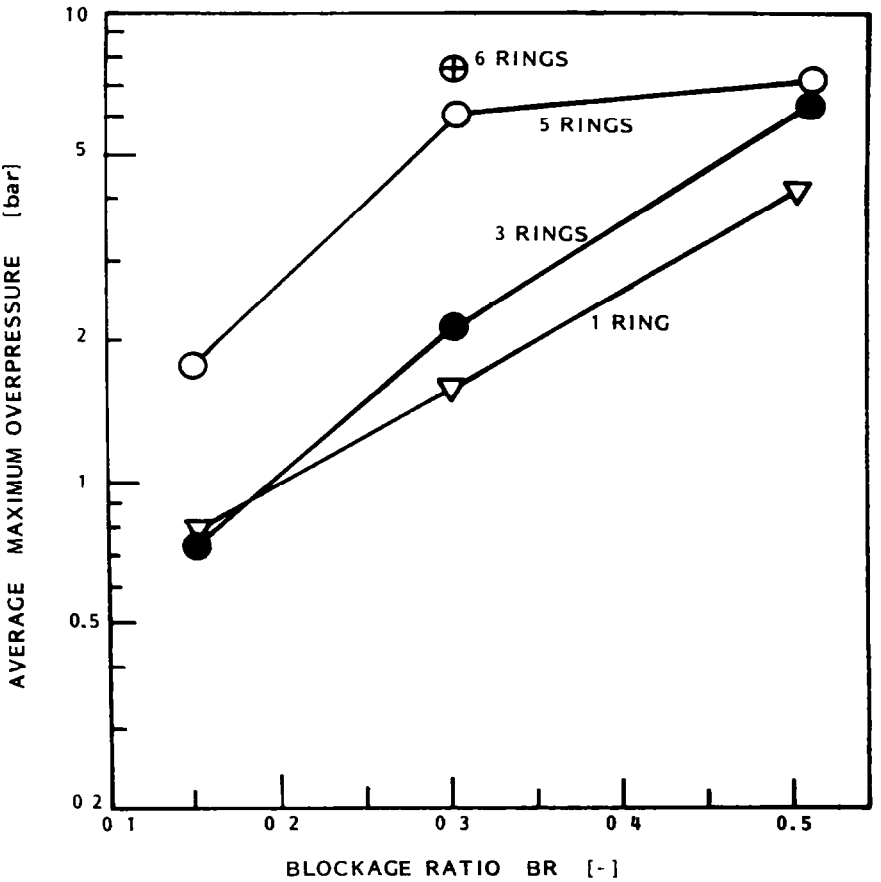

Fig 3 Average maximum overpressure near the ignition end (x = 0 8 m), in the middle (x = 4 8 m) and near the open end (x = 9 6 m) as function of blockage ratio, $BR = 1 - (d/D)^2$ Propane—air mixtures

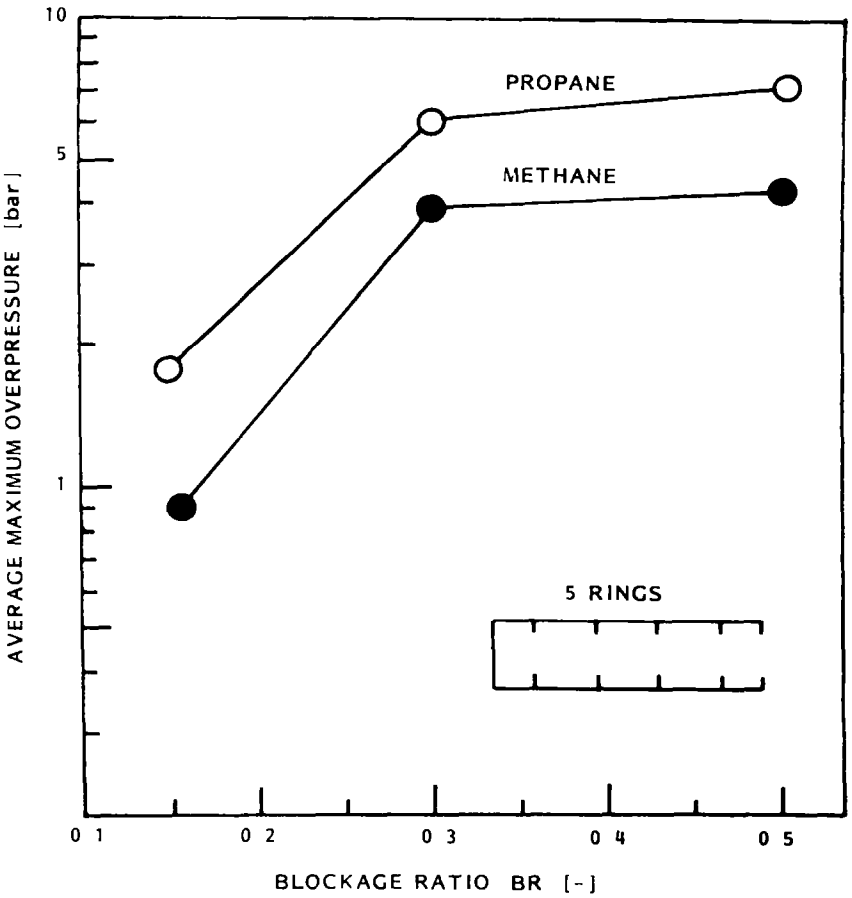

Fig 4 Comparison of average maximum overpressure for propane and methane (Moen et al [5]) for different blockage ratios

corresponding pressures for methane—air were 4 0 bar, 0 39 bar and 4 3 bar, respectively

Figure 3 shows the variation of average maximum overpressure with blockage ratio with the number of rings as parameter The trend is the same as that reported for methane—air by Moen et al [5] A strong variation with blockage ratio can be observed Also, increasing the number of rings increases the average maximum pressure in the tube Figure 4 shows a comparison of the maximum average overpressure versus blockage ratio between methane and propane Pressure differences by a factor of approximately 2 can be seen for all three blockage ratios tested

Peak overpressure in the tube as function of number of rings is shown in Fig 5 This figure shows that 5 rings of blockage ratio 0 16 exhibit the same peak overpressure as 1 ring with a blockage ratio equal to 0 3 A decrease in pressure with increasing number of orifice plates as observed with methane was not found with propane

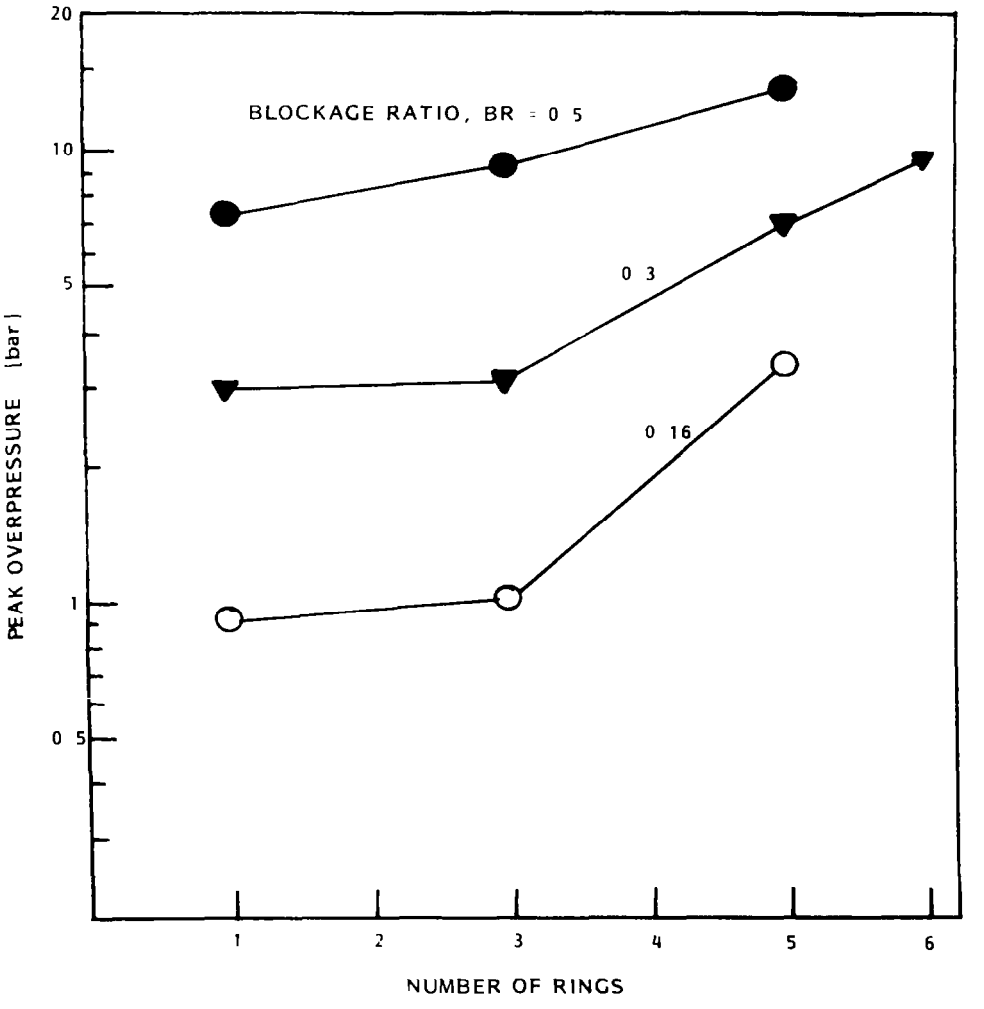

Fig 5 Peak overpressure inside the tube as function of number of rings for blockage ratios BR = 0 16, 0 3 and 0 5 Propane—air mixtures

The terminal flame speed in the tube versus number of rings is shown in Fig 6 Here the terminal flame speed is taken to be the average centre line flame speed over the last 3 m of the 10 m of total flame travel The figure shows a steady increase of flame speed with number of rings for the blockage ratios BR = 0 16 and 0 5, whereas there is a maximum flame speed at 5 rings for the blockage ratio 0 3 The flame speed for the blockage ratio 0 5 is smaller for 1, 3 and 5 rings than for blockage ratio 0 3 This suggests that an optimum flame speed exists at a given number of rings and a given blockage ratio

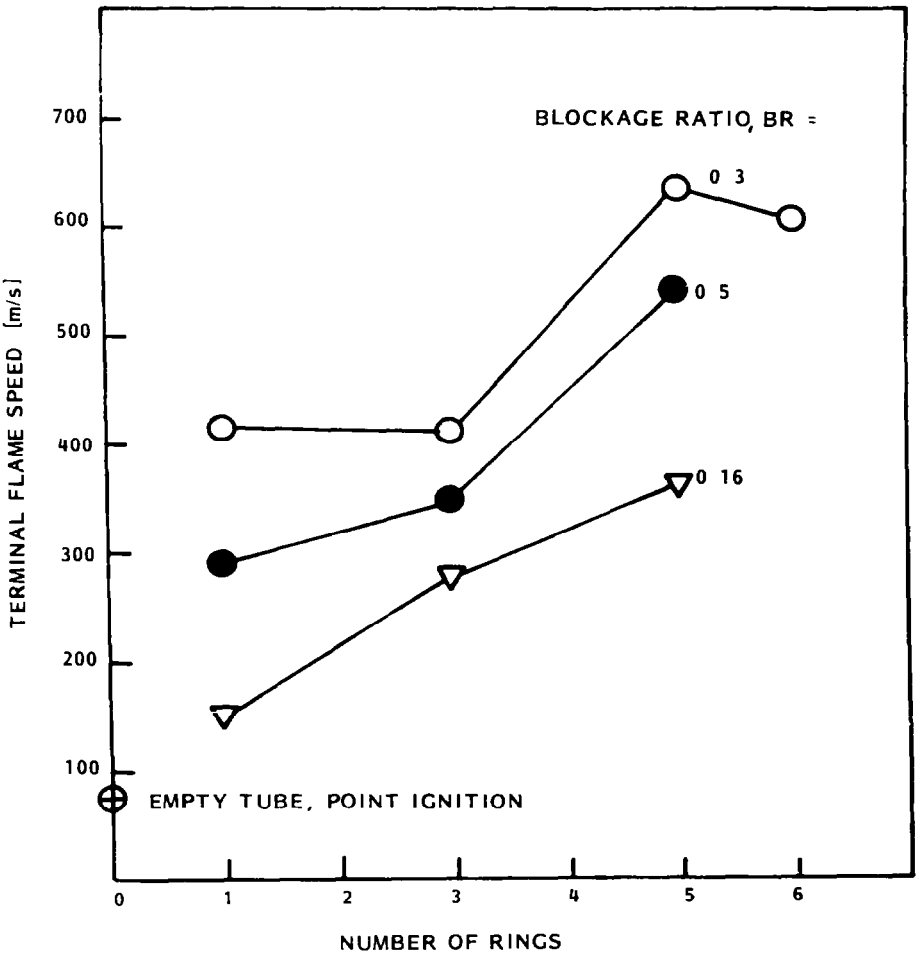

Fig 6 Terminal flame speed (between x_s = 6 61 m and x_s = 9 61 m) versus number of rings for various blockage ratios Propane—air mixtures

Figure 7 shows the time of arrival of the flame versus distance from ignition along the centre line and along the shear layers of the orifice rings The figure shows three different tests with the same geometry and mixture conditions and gives the degree of repeatability of the flame propagation process An interesting finding is depicted in Figs. 7b and c These show that the flame at the shear layer behind a ring accelerates so fast that the flame at the centre line leaves the tube exit later than at the shear layer This suggests, as also shown by the prediction method of Hjertager [7] that the largest rates

Fig 7 Time—distance plots of the flame propagation along the centre line and along the shear layers for three different tests in the same geometry BR = 0 3 and 5 rings Propane—air mixtures

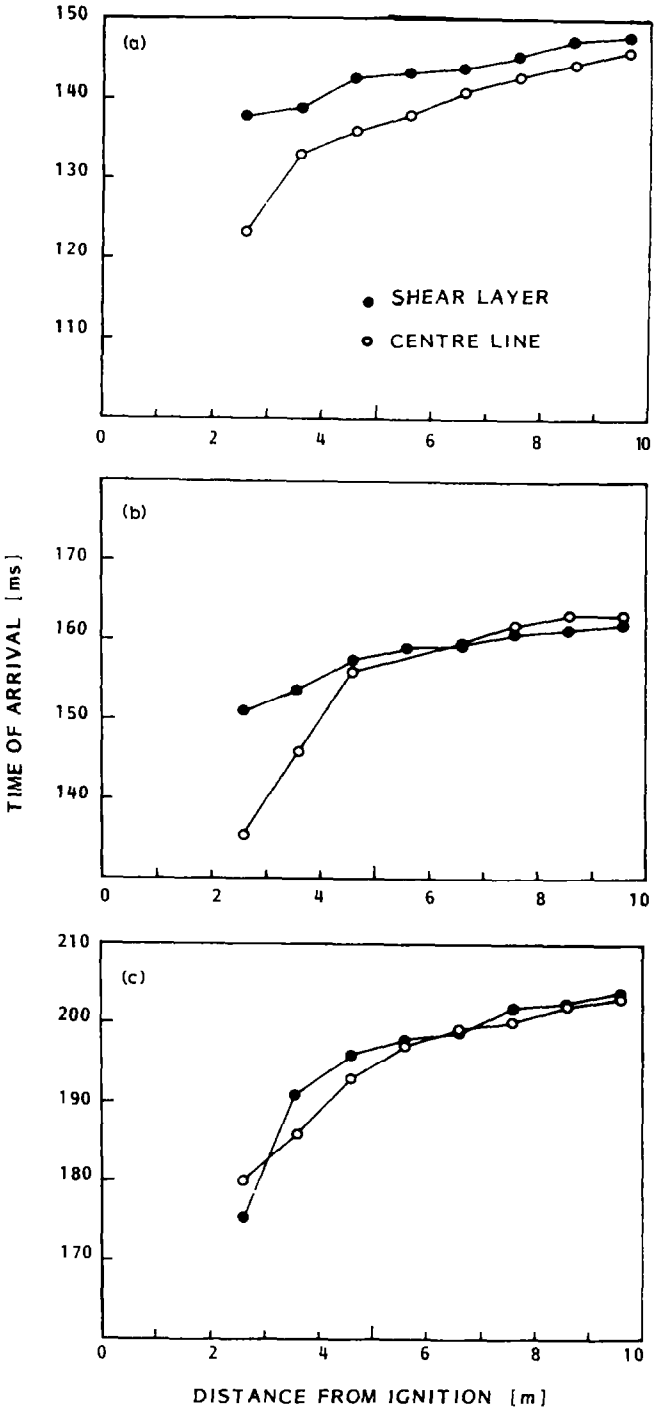
(a)
150
140
130
120
110
SHEAR LAYER
CENTRE LINE
0
2
4
6
8
10
(b)
170
160
150
140
(c)
210
200
190
180
170
TIME OF ARRIVAL [ms]
DISTANCE FROM IGNITION [m]

of combustion occur in the shear layers Figure 7 also shows the same trend as was found for methane by Moen et al [5], namely that the maximum centre-line terminal flame speed is reached before the flame has travelled halfway down the tube length This is also the general result from most of the geometrical arrangements which were tested

It has become evident that the largest rates of combustion occur in localized volumes behind the ring obstacles In order to explain some of the observed properties of flame propagation it is important to establish some characteristics of these volumes or rather mixing layers From the theory of simple mixing layers (Bradshaw [11]) it is known that the thickness varies linearly with distance from the origin Also, it is known that the largest gradients are found at the start, and then gradually decrease along the flow path This again implies that turbulence is large close to the origin and then decays, because turbulence velocity is approximately proportional to the gradient of the velocity field It is therefore possible to estimate the turbulence-influenced regions of the flow as a ring torus with triangular cross-section stretching from one obstacle to the next Thus we may estimate the total volume as

$$V_t \approx p^2 d(U_c/u_t)^2 n$$

where p is the pitch, d the inner diameter of the ring orifices, U_c the flow velocity in the center of the ring passage, u_t the turbulence velocity and n the number of obstacles

From the above expression it is seen that when the inner diameter is decreased, the volume also decreases This means that, for choked flow through the ring orifices, the integrated rates of reaction should decrease, thus reducing the pressure generated by combustion But on the other hand, as the blockage ratio increases, the pressure drop due to flow through the orifice will also increase This suggests, as shown in Figs 3 and 4, that the pressure produced by increasing the blockage ratio seems to level off

For a given blockage ratio, an increase of number of plates also increases the pressure to some level If we again look at the turbulence-influenced volume expressed as

$$V_t \sim L^2/nd(U_c/u_t)^2$$

we observe that increasing the number of plates, n, along a given length of flame travel, L, diminishes the volume This indicates that an increase of number of plates may decrease the combustion-produced pressure This is found in the methane—air experiments by Moen et al [5] and is reproduced in Fig 8 For the propane—air experiments this decrease in produced pressure was not observed This can be explained by the difference in ignition delay times between the two fuels Methane—air will ignite at a longer distance from the obstacles than the propane—air Thus, for the same total shear layer volume in the tube, more of this volume will burn for propane as compared with methane

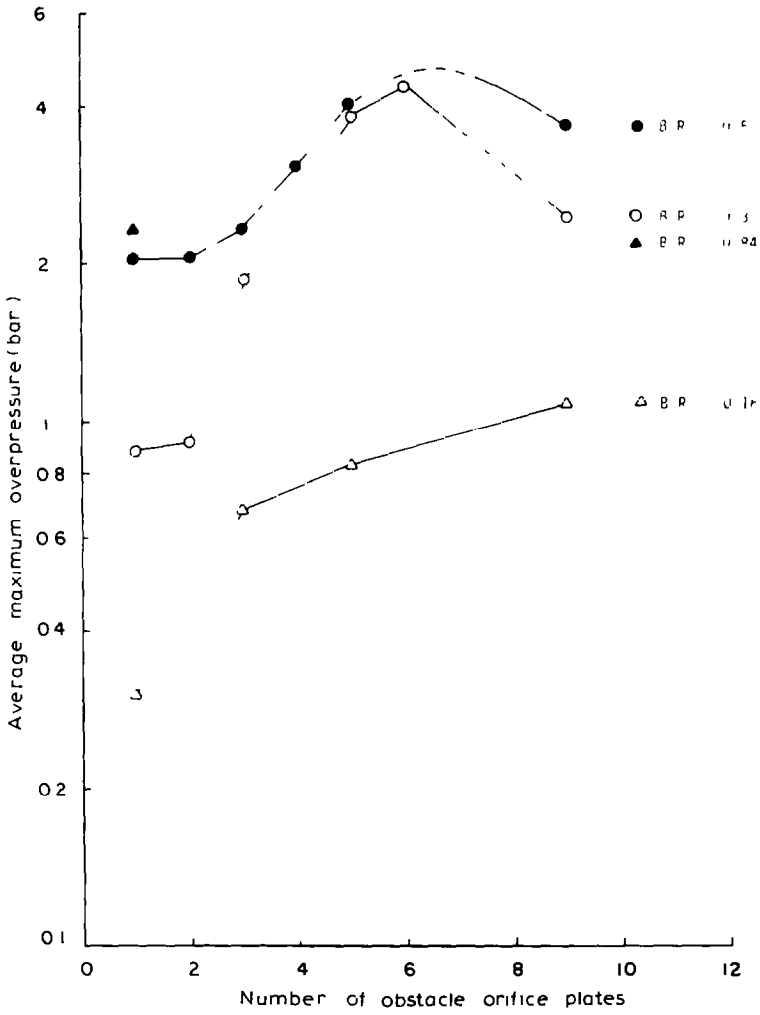

Fig 8 Average of maximum pressure near the ignition end, in the middle, and near the open end of the tube for different number of obstacles with various blockage ratios One obstacle at x = 5 13 m, two obstacles at x = 5 13, 9 33 m for BR = 0 3, and x = 1 65, 5 13 m for BR = 0 5 Methane—air mixtures (Moen et al [5])

The data given above are all for homogeneous stoichiometric mixtures Hjertager et al [12] have recently conducted a large-scale study using homogeneous clouds with variable stoichiometry Figure 9 shows the results for peak pressures in methane—air mixtures as function of concentration of methane The results show that the pressure maximizes at slightly rich mixtures and there is a drop towards richer and leaner mixtures The limits for propagation are found to be 6% on the lean side and 14% on the rich side This is somewhat narrower than the standard 5%, 15% flammability limits

This difference is probably brought about by the fact that turbulence makes propagation more difficult towards the limits as shown by Ballal and Lefebvre [13] Figure 10 shows similar data for propane—air The limits to propagation are 2 3% and 7 9%

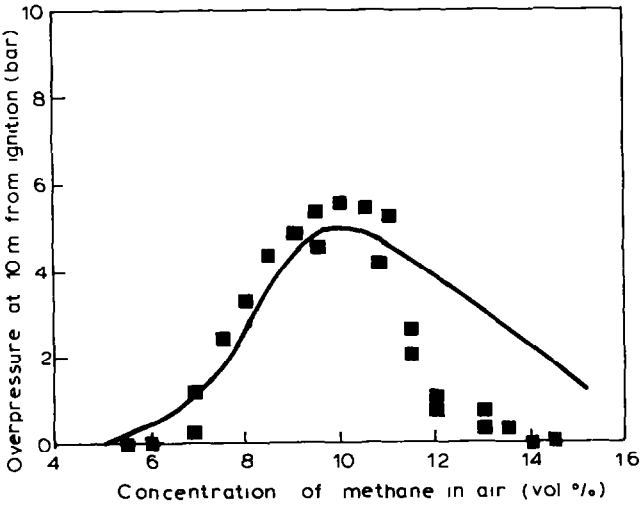

Fig 9 Comparison of measured (▪, Raufoss in Ref [12]) and predicted (—) peak over pressures at the exit of the 50 m³ tube versus concentration of methane

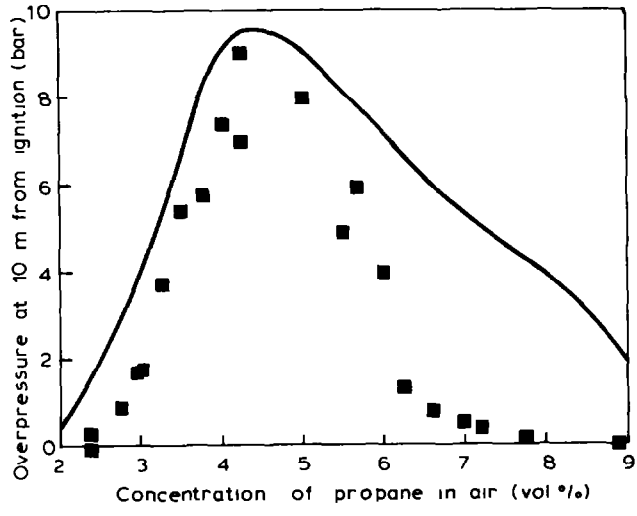

Fig 10 Comparison of measured (▪, Raufoss in Ref [12]) and predicted (—) peak overpressures at the exit of the 50-m³ tube versus concentration of propane

3 3 Influence of mode of propagation

All the experimental data discussed so far have focused attention on the axial mode of propagation Bjørkhaug and Hjertager [14] have performed a study with one objective, to investigate the influence of propagation mode Figure 11 shows a comparison between the axial mode given by Chan et al [15] and the results for the cylindrical mode [14] The figure shows that the pressures generated are smaller in the cylindrical mode than in the axial mode However, this difference diminished as the length of flame travel was increased, i e , for a 0 5 m flame travel the peak pressure ratio is 4 1, and for 1 m flame travel the ratio is 1.7 1 Thus it is important to obtain data for increased length of flame propagation to reveal the differences, if any, for larger scale situations

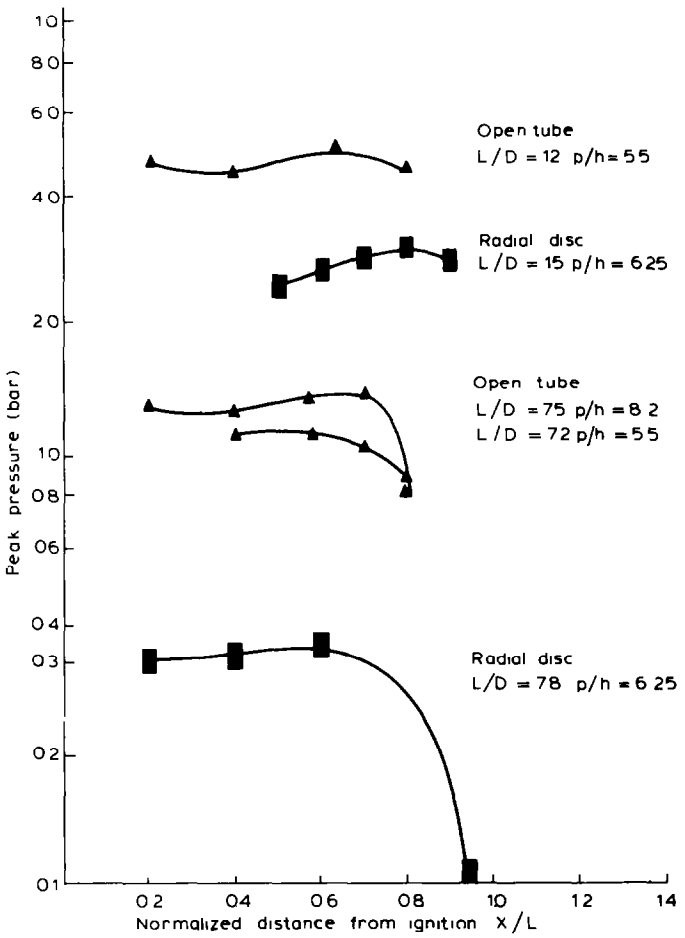

Fig 11 Comparison of maximum pressure at various positions for experiments with axial flame propagation [15] and radial flame propagation [14] in methane—air mixtures

Turbulent flame propagation data in the spherical mode are scarce Lind and Whitson [16] did some tests in balloons of diameter 5 and 10 m without obstacles, but they obtained flame speeds only in the order of 10 m/s Their results indicate that freely propagating spherical flames do not produce high flame speed even in large-scale experiments However, data on spherical flames with obstacles are needed to obtain good knowledge of the influence of propagation mode in obstacle-accelerated flames

Hjertager et al [12] did some experiments with a point-source ignition in the 50 m^3 tube and compared this with the planar ignition data given above It turned out that the pressures produced were reduced by a factor of approximately two as compared to the data given in Figs 9 and 10 This was explained by the fact that the initial phases of flame propagation were different In Figs 9 and 10 the flame was in the axial mode right from the start,

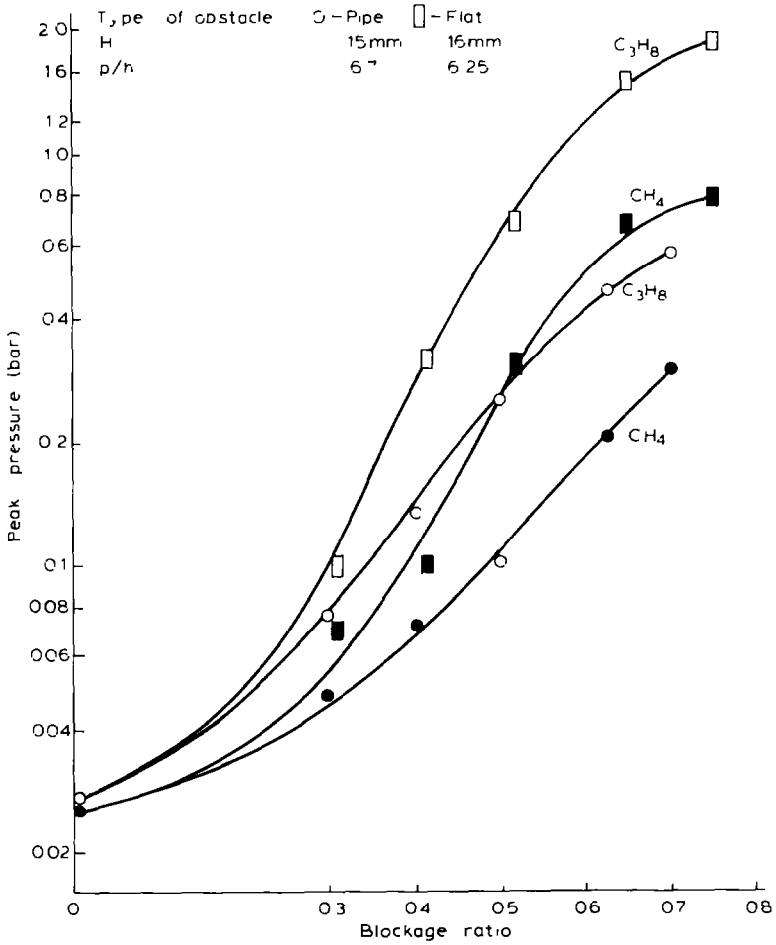

Fig 12 Maximum pressure in radial disc experiments versus blockage ratio for various obstacle shapes (Bjørkhaug and Hjertager [14])

whereas the point-source-ignited explosions started in the spherical mode and were forced to the axial mode by the bounding walls after the initial phase of propagation

3 4 Influence of obstacle shape

The obstacles in the experiments described above were all sharp edged Bjørkhaug and Hjertager [14] also investigated the influence of obstacle shape on the flame and pressure development in a radial vessel (cylindrical propagation mode) Two types of obstacle shapes were tested, namely sharp edged and circular obstacles Figure 12 gives the results as peak pressures produced in the vessel as a function of blockage ratio We can see that there is a distinct difference for both fuels tested between the two obstacle shapes Sharp-edged obstacles produce approximately two times as high a pressure as circular obstacles for the same blockage ratio and number of obstacles along the propagation path Another interesting finding in Fig 12 is that the difference between the two fuels, methane and propane, is the same in this small-scale vessel as in the large-scale data shown in Fig 4 This indicates that the differences in pressure are brought about by the turbulence, since the laminar flame propagation velocities are similar for methane and propane

4 Numerical studies

4 1 General

Gas explosion hazard assessments in flammable gas handling operations are crucial in obtaining an acceptable level of safety In order to perform such assessments good predictive tools are needed, which take account of the relevant parameters, such as geometrical design variables and gas cloud distribution A theoretical model must therefore be tested against sufficient experimental evidence prior to becoming a useful tool The experimental data should include both variations in geometry and gas cloud composition and the model should give reasonable predictions without use of geometry- or case-dependent constants

It has in the past been usual to predict the flame and pressure development in vented volumes by modelling the burning velocity of the propagating flame This may be successful if we have a simple-mode flame propagation such as axial, cylindrical or spherical propagation in volumes without obstructions in the flow If these are present, however, it is almost impossible to track the flame front throughout complex geometries It has been apparent that in these situations it is more useful to model the propagation by calculating the rate of fuel combustion at different positions in the volume It is also important to have a model which is able both to model subsonic and supersonic flame propagation to enable a true prediction of what can happen in an accident scenario One such model, which in principle meets all these needs, has been proposed by the present author [7, 8] The model has been tested against various experimental data from homogeneous stoichiometric

methane—air and propane—air mixtures in both large-scale and small-scale geometries The remainder of this paper will review the simulation model, show some validation calculations and present some predicted scaling characteristics

4 2 Basic equations

The problem of turbulent explosion can be handled by solving for the time evolution of time mean values of the dependent quantities in the domain of interest The time mean of a variable varying with time, t, may be expressed as

$$\Phi(t) = \frac{1}{T} \int_{t}^{t+T} \hat{\Phi}(t+\tau)\mathrm{d}\tau \tag{1}$$

where $\Phi(t)$ is the time mean value of the instantaneous value $\hat{\Phi}(t)$ averaged over the time interval T T must satisfy two competing demands Firstly, it must be small enough not to smear out the sought time dependence of the system under consideration Secondly, it must be large enough to be able to produce sufficient information to enable relevant time mean values in the interval This means time mean values of both the relevant quantities and their second order correlations must be obtainable in the time interval T This is often possible since, conversely, turbulence has higher frequencies than the large-scale motion which generates turbulence The equation of motion and energy can thus be expressed in tensor notation as

$$\frac{\partial \rho}{\partial t} + \frac{\partial}{\partial x_i}(\rho U_i) = 0 \tag{2}$$

$$\frac{\partial}{\partial t}(\rho U_i) + \frac{\partial}{\partial x_j}(\rho U_j U_i) = -\frac{\partial p}{\partial x_i} + \frac{\partial}{\partial x_j}(\sigma_{ij}) \tag{3}$$

$$\frac{\partial}{\partial t}(\rho h) + \frac{\partial}{\partial x_j}(\rho U_j h) = -\frac{\partial}{\partial x_j}(J_{h,j}) + \frac{Dp}{Dt} + S_h \tag{4}$$

Here U_i is the velocity component in the x_i coordinate direction, p is the pressure, ρ is the density, h is the enthalpy and σ_{ij} and $J_{h,j}$ are the fluxes of momentum and energy

The combustion is treated as a single-step irreversible reaction with finite reaction rate between fuel and oxydant Hence, the reaction scheme may be written as

$$1 \text{ kg fuel} + s \text{ kg oxygen} \rightarrow (1+s) \text{ kg products} \tag{5}$$

Here s is the stoichiometric oxygen requirement to burn 1 kg of fuel This simple reaction scheme results in mixture composition being determined by solving for only two variables, namely mass fraction of fuel, m_{fu}, and the

mixture fraction, f

$$\frac{\partial}{\partial t}(\rho m_{\mathrm{fu}}) + \frac{\partial}{\partial x_j}(\rho U_j m_{\mathrm{fu}}) = -\frac{\partial}{\partial x_j}(J_{\mathrm{fu},j}) + R_{\mathrm{fu}} \tag{6}$$

$$\frac{\partial}{\partial t}(\rho f) + \frac{\partial}{\partial x_j}(\rho U_j f) = -\frac{\partial}{\partial x_j}(J_{f,j}) \tag{7}$$

Here R_{fu} is the time mean rate of combustion of fuel, whereas $J_{\mathrm{fu},j}$ and $J_{f,j}$ are the diffusive fluxes in the x_j direction The basis for this to be valid is that the Schmidt numbers are equal for all species, an approximation which is often found in turbulent flows

The mixture fraction is defined as

$$f = \frac{\beta - \beta_\infty}{\beta_0 - \beta_\infty} \tag{8}$$

where β is a conserved combined variable of, for example, mass fraction of fuel, m_{fu} and mass fraction of oxygen, m_{O_2}, expressed as

$$\beta = m_{\mathrm{fu}} - m_{\mathrm{O}_2}/s \tag{9}$$

β_0 is the value of β at a fuel-rich reference point, for example a fuel leakage point in the domain, and β_∞ is the value of β at an oxidant-rich reference point, for example the ambient air condition For a homogeneous premixed system the mixture fraction will be constant in the domain of interest and, consequently, only the m_{fu} equation needs to be solved

To solve the governing equations, eqns (2)—(7) given above, the fluxes, $J_{\Phi,j}$, and the rate of combustion, R_{fu}, have to be specified, together with relevant boundary and initial conditions Both the fluxes and the combustion rate are time mean averaged values of fluctuating quantities The fluxes can, for a general scalar variable Φ, and a velocity component U_j, be expressed

$$J_{\Phi,j} = -\rho\overline{u_j\phi} \tag{10}$$

and

$$\sigma = -\rho\overline{u_i u_j} \tag{11}$$

where u_i and ϕ are the instantaneous fluctuations around the time mean values U_j and Φ, respectively The overbar indicates time mean value over the time interval T as defined in eqn (1) When specifying the correlations given in eqns (10) and (11) it is usual to relate these to the product of time mean gradients of the relevant variables and an effective turbulent transport coefficient For a general scalar variable Φ and a velocity component U_j the relations are

$$J_{\Phi,j} = -\frac{\mu_{\mathrm{eff}}}{\sigma_\Phi}\frac{\partial \Phi}{\partial x_j} \tag{12}$$

and

$$\sigma_{ij} = \mu_{\text{eff}} \left(\frac{\partial U_i}{\partial x_j} + \frac{\partial U_j}{\partial x_i} \right) - \frac{2}{3} \delta_{ij} \left(\rho k + \mu_{\text{eff}} \frac{\partial U_k}{\partial x_k} \right) \tag{13}$$

respectively

Here $\delta_{ij} = 1$ if $i = j$ and $\delta_{ij} = 0$ if $i \neq j$ An effective turbulence viscosity, μ_{eff}, and the kinetic energy of turbulence have been introduced in the above expressions, together with an effective Prandtl/Schmidt number, σ_Φ The kinetic energy of turbulence, k, is related to the fluctuating turbulence velocity components in the three coordinate directions as

$$k = \frac{1}{2} (\overline{u_1^2} + \overline{u_2^2} + \overline{u_3^2}) \tag{14}$$

The effective turbulence viscosity is given by the two turbulence parameters, the isotropic turbulence velocity, u_t, and a length scale, l, as

$$\mu_{\text{eff}} = \mu_l + \rho u_t l \tag{15}$$

μ_l is the molecular viscosity The determination of the turbulence velocity and length scale is done by use of a turbulence model

4 3 Turbulence modelling

The determination of u_t and l is done by application of the so-called k—ϵ model of turbulence [17] The turbulence velocity is related to the kinetic energy of turbulence, k, as

$$u_t = \left(\frac{2}{3} k \right)^{1\,2} \tag{16}$$

and the length scale, l, is related to the kinetic energy of turbulence, k, and its rate of dissipation, ϵ, as

$$l \sim \frac{k^{3\,2}}{\epsilon} \tag{17}$$

Inserting eqns (16) and (17) into expression (15) gives

$$\mu_{\text{eff}} = \mu_l + C_D \rho \frac{k^2}{\epsilon} \tag{18}$$

C_D is a constant taken to be 0 09 [17]

The conservation equations that determine the distribution of k and ϵ read

$$\frac{\partial \rho k}{\partial t} + \frac{\partial}{\partial x_j} (\rho U_j k) = \frac{\partial}{\partial x_j} \left(\frac{\mu_{\text{eff}}}{\sigma_k} \frac{\partial k}{\partial x_j} \right) + G - \rho \epsilon \tag{19}$$

$$\frac{\partial \rho \epsilon}{\partial t} + \frac{\partial}{\partial x_j} (\rho U_j \epsilon) = \frac{\partial}{\partial x_j} \left(\frac{\mu_{\text{eff}}}{\sigma_\epsilon} \frac{\partial \epsilon}{\partial x_j} \right) + C_1 \frac{\epsilon}{k} G - C_2 \rho \frac{\epsilon^2}{k} \tag{20}$$

The two new constants appearing above, C_1 and C_2, are given the values 1 44 and 1 79, respectively [17] The Schmidt numbers, σ_k and σ_ϵ, are given the values 1 0 and 1 3, respectively, whereas the other Schmidt/Prandtl numbers are put equal to 0 7 The generation rate of turbulence is given by

$$G = \sigma_{ij} \frac{\partial U_j}{\partial x_i} \tag{21}$$

These production rate terms take account of turbulence produced by shear and compression/expansion If buoyancy production or Rayleigh—Taylor instability production is important, additional terms may be added Such terms have recently been proposed

4 4 Combustion modelling

For the simple reaction scheme given in eqn (5) above, an instantaneous rate of reaction can be written as

$$\hat{R}_{\mathrm{fu}} = -\rho^2 \hat{k}_{\mathrm{fu}} \hat{m}_{\mathrm{fu}} \hat{m}_{\mathrm{O}_2} \tag{22}$$

Here k_{fu} is the instantaneous value of the Arrhenius temperature dependence of the rate constant If this rate constant and the mass fractions are written as the sum of a time mean and a fluctuating quantity ($\hat{m}_i = m_i + m_i'$), the reaction rate (ignoring density fluctuations) would be written as

$$\hat{R}_{\mathrm{fu}} = -\rho^2 (k_{\mathrm{fu}} + k'_{\mathrm{fu}})(m_{\mathrm{fu}} + m'_{\mathrm{fu}})(m_{\mathrm{O}_2} + m'_{\mathrm{O}_2}) \tag{23}$$

Multiplying out this expression and taking the time mean value of the result gives

$$R_{\mathrm{fu}} = -\rho^2 (k_{\mathrm{fu}} m_{\mathrm{fu}} m_{\mathrm{O}_2} + k_{\mathrm{fu}} \overline{m'_{\mathrm{fu}} m'_{\mathrm{O}_2}} + m_{\mathrm{fu}} \overline{k'_{\mathrm{fu}} m'_{\mathrm{O}_2}} + m_{\mathrm{O}_2} \overline{k'_{\mathrm{fu}} m'_{\mathrm{fu}}} + \overline{k'_{\mathrm{fu}} m'_{\mathrm{fu}} m'_{\mathrm{O}_2}}) \tag{24}$$

The above relation shows that even the simplest reaction scheme gives rise to a rather complicated expression for the time mean reaction rate This indicates that rigorous mathematical models of the reaction rate based on chemical kinetics in turbulent situations have immense obstacles prior to providing solutions It is therefore necessary to seek, if possible, alternative and simpler methods

Experiments have shown that rate of combustion in flames is mainly dependent on hydrodynamic parameters This implies that combustion rate is limited by the rate of molecular mixing between the reactants This mixing is directly linked to the rate at which turbulent eddies are dissipated For a scalar variable this dissipation is formally expressed as

$$\epsilon_\Phi = D_\Phi \overline{\frac{\partial \Phi}{\partial x_k} \cdot \frac{\partial \Phi}{\partial x_k}} \tag{25}$$

D_Φ is the molecular diffusion coefficient The hydrodynamic rate of dissipation of turbulent kinetic energy is denoted by ϵ It is therefore assumed that

combustion rate is proportional to the rate of dissipation of kinetic energy of turbulence

$$R_{fu} = -\rho\epsilon \frac{g_\Phi^{1/2}}{k} \tag{26}$$

g_Φ is the variance of the fluctuations of the limiting species in question Magnussen and Hjertager [18] argue that the fuel, oxidant and reaction products appear as intermittent fluctuating quantities Consequently, the fluctuating species may be related to time mean values of fuel, oxidant or reaction products Therefore

$$R_{fu} = -A\rho \frac{\epsilon}{k} m_{lim} \tag{27}$$

where m_{lim} is the smallest of the three mass fractions, namely fuel, m_{fu}, oxygen, m_{O_2}/s, or mass fraction of fuel already burnt, $m_{fu,b}$ A is a constant In order for eqn (27) to be valid, the chemical kinetics of the system under consideration must be fast In many cases this is not the case, especially in the fast transient combustion which for example occurs in high-speed gas explosions A simple modification of the above expression has therefore been proposed [8]

Based on the chemical kinetics of the system, a chemical time can be defined, τ_{ch} Also, the lifetime of the turbulent eddies can be defined, τ_e Ignition or extinction is assumed to occur when these two times are in a given ratio, namely

$$\tau_{ch}/\tau_e = D_{ie} \tag{28}$$

The following modification to the rate expression in eqn (27) is therefore used

$$\begin{aligned} &- \text{if } \tau_{ch}/\tau_e \geqslant D_{ie} \qquad \text{then } R_{fu} = 0 \\ &- \text{if } \tau_{ch}/\tau_e < D_{ie} \qquad \text{then } R_{fu} = -A\rho \frac{\epsilon}{k} m_{lim} \end{aligned} \tag{29}$$

The above criterion is closely related to the models proposed by Radhakrishnan et al [19] and Magnussen [20] for extinction phenomena The eddy lifetime or mixing time is defined as

$$\tau_e = \frac{l}{u_t} \sim \frac{k}{\epsilon} \tag{30}$$

The chemical time is taken equal to the chemical induction time which is often expressed as

$$\tau_{ch} = A_{ch} \exp(E/RT)(\rho m_{fu})^a (\rho m_{O_2})^b \tag{31}$$

Radhakrishnan et al. [19] proposed that the chemical time should be taken equal to the time for a laminar flame to propagate across a length equal to

the Taylor micro scale, λ Their application, however, was a correlation of blow-off velocity data in disc-stabilized premixed flames

4 5 Solution procedure

It is noted that all conservation equations mentioned above can be written in the following general form

$$\underset{\text{I}}{\frac{\partial}{\partial t}(\rho\Phi)} + \underset{\text{II}}{\frac{\partial}{\partial x_j}(\rho U_j\Phi)} = \underset{\text{III}}{\frac{\partial}{\partial x_j}\left(\Gamma_\Phi \frac{\partial\Phi}{\partial x_j}\right)} + \underset{\text{IV}}{S_\Phi} \tag{32}$$

This means, equations with four distinct terms, namely I, transient, II, convection, III, diffusion, and IV, source terms

Solution of these equations is performed by finite-domain methods Details of the computation method are given by Hjertager [7] Only a brief description is given here

The calculation domain is divided into a finite number of main grid points where pressure, p, density, ρ, mass fraction of fuel, m_{fu}, mixture fraction, f, and the two turbulence quantities, k and ϵ, are stored The three velocity components, U, V and W, are, on the other hand, stored at grid points located midway between the main points The conservation equations are inte grated over control volumes surrounding the relevant grid points in space and over a time interval, Δt This integration is performed using upwind differencing and implicit formulation

The result of this is a set of non-linear algebraic equations, which are solved by application of the well-known tri-diagonal matrix algorithm used along the three coordinate directions Special care has been taken to solve the pressure/velocity/density coupling of the three momentum equations and the mass balance The "SIMPLE" method developed by Patankar and Spalding [21] for three-dimensional incompressible parabolic flow has been extended by Hjertager [7] to compressible flows and is used to handle this coupling The method introduces a new variable, the so-called pressure correction, which makes the necessary corrections to the velocity components, pressure and density to make them obey the mass balance constraint at the new time level The pressure correction is determined by solution of a set of algebraic equations derived from the linearized momentum equations and the mass balance equation

4 6 Validation calculations

Tube

Calculations of flame and pressure development have been performed for two different homogeneous fuel—air mixtures contained in a tube geometry and in a planar vented channel

The methane—air and propane—air data [5, 6, 12] used are taken from a large-scale explosion study in a 50-m^3 tube of 2 5 m diameter and 10 m

length with 5 orifice rings with variable blockage ratios The chemical times are taken from Burcat et al [22] and Schott and Kinsey [23], and the relevant parameters used in eqn (31) are compiled in Table 1

Figure 13 shows a comparison between experiments and predictions of

TABLE 1

Values of parameters in eqn (31) for various fuels

Fuel	A_{ch}	a	b	E/R	Reference
Methane	$3\,62 \times 10^{14}$	0 33	−1 03	23 300	Burcat et al [22]
Propane	$4\,40 \times 10^{14}$	0 57	−1 22	21 210	Burcat et al [22]
Hydrogen	$2\,25 \times 10^{-11}$	0	−1 0	9 132	Schott and Kinsey [23]

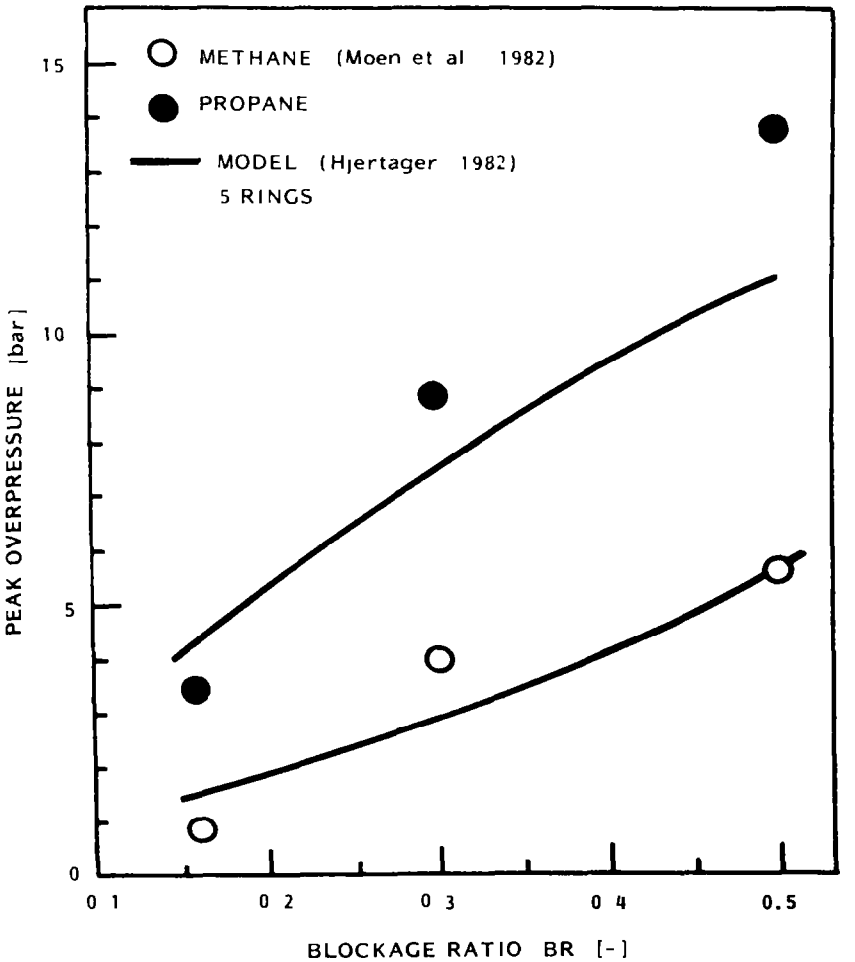

Fig 13 Peak measured [4, 5] and predicted pressures in the 50-m³ combustion tube as function of blockage ratio, $BR = 1 - (d/D)^2$ Propane—air and methane—air mixtures

peak pressures versus blockage ratio ($BR = (1 - (d/D)^2)$ for methane—air and propane—air mixtures The figure shows that the large difference in peak pressures between methane—air and propane—air explosions is fairly well predicted The present prediction method also gives the correct behaviour of pressure versus blockage ratio There is, however, some underprediction for propane—air at blockage ratio 0 5 It should also be mentioned that the original combustion rate model [18] would only show a 20 percent difference between methane and propane This clearly demonstrates that changes in thermodynamic properties and the infinite chemical kinetics assumption are not alone capable of reproducing the experimental differences between methane—air and propane—air explosions

Figure 14 shows a comparison between the computation model and the

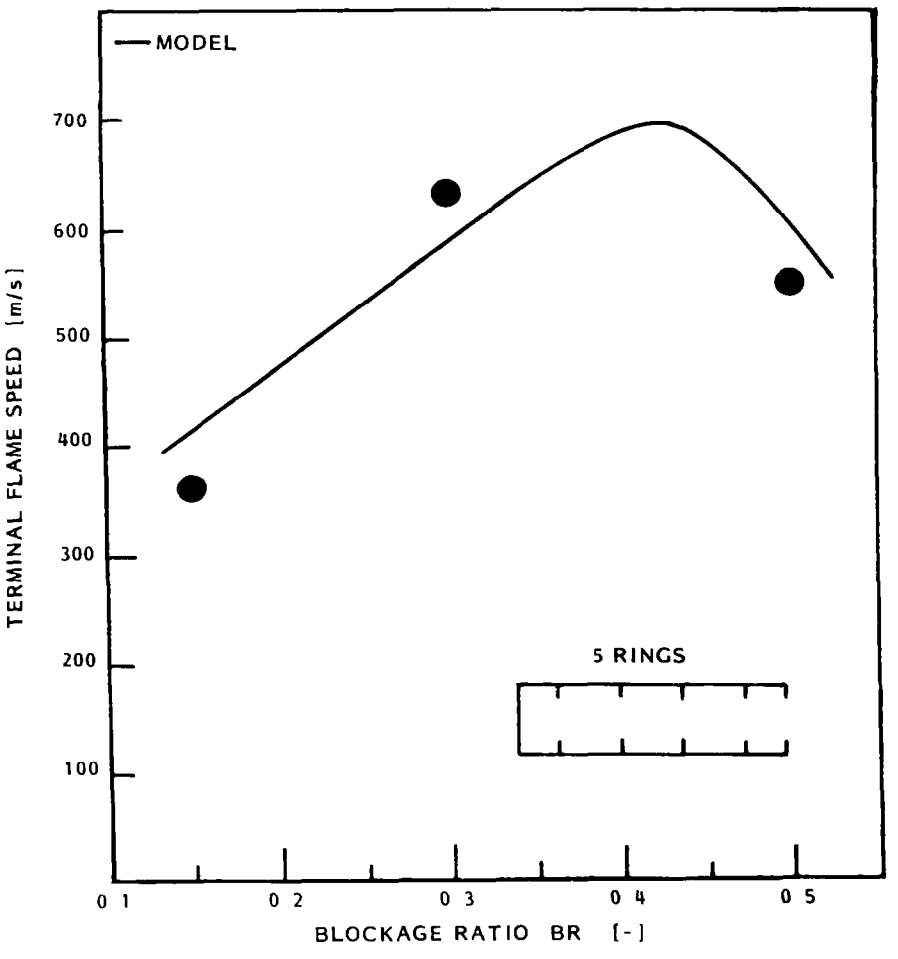

Fig 14 Comparison between measured (Hjertager et al [6]) and predicted variations of terminal flame speed with blockage ratio

experiments of the terminal flame speed for propane—air as function of blockage ratio It is seen that the agreement is satisfactory and that the model predicts the optimum flame speed at a blockage ratio equals approximately 0 4

Figures 9 and 10 show a comparison between predicted and measured peak pressures for variable concentrations of methane—air and propane—air explosions in the 50-m^3 tube Good agreement between predictions and experiments can be observed for lean mixtures of methane—air and propane—air, whereas less agreement is seen for both gases at the rich side of stoichiometry There is good correspondence between measured and predicted concentration for optimum pressure build-up Both mixtures exhibit this maximum at slightly rich mixtures This is the same trend as found in detonation

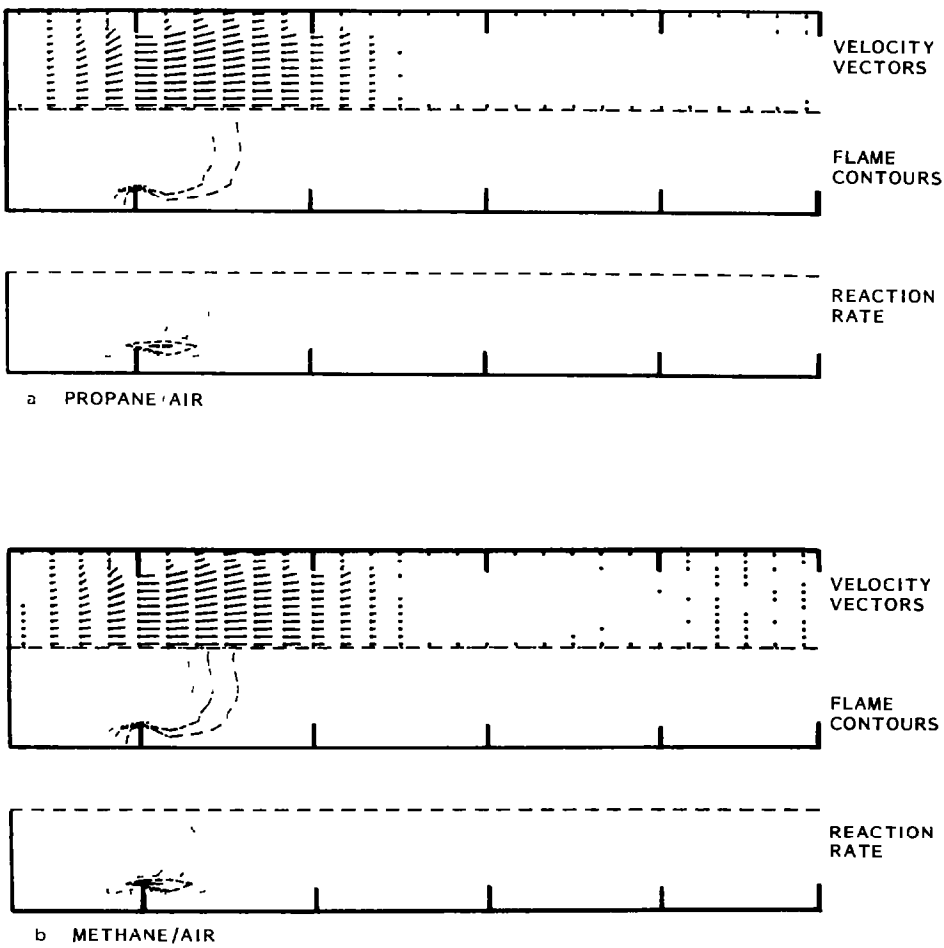

Fig 15 Distribution of velocity, flame and reaction rate for (a) propane—air and (b) methane—air explosions after the flame has passed the first obstacle

sensitivity studies in both methane—air and propane—air mixtures [10] The predicted maximum peak pressures are approximately 5 bar for methane and 9 5 bar for propane This difference has come about mainly because of different reaction times Figures 15 and 16 elucidate this in more detail These figures show local distributions within the tube of velocity, flame contours and reaction rate contours for both fuels In Figs 15a and b the conditions after the flame has passed the first obstacle are shown We can see that the local distributions of all variables are almost identical for both gases However, in Figs 16a and b, which show the situation after the flame has propagated over the second obstacle, some differences can be observed At this position of the flame the turbulent mixing time, τ_e, has diminished to a value which corresponds to quenching in some regions where the shear in the

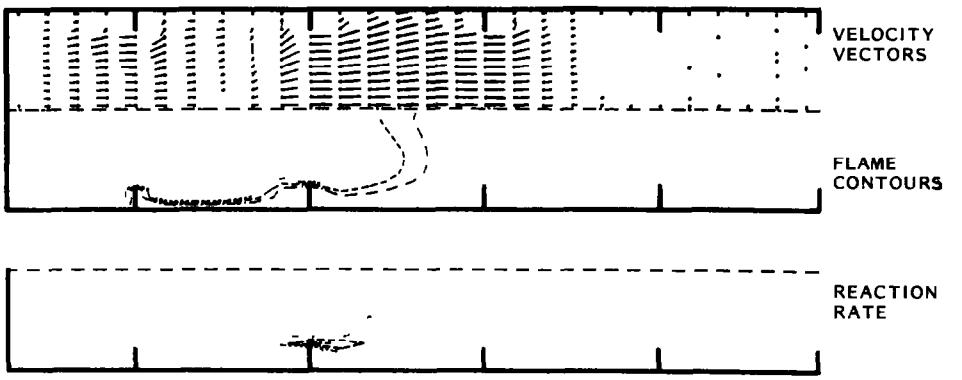

a PROPANE/AIR

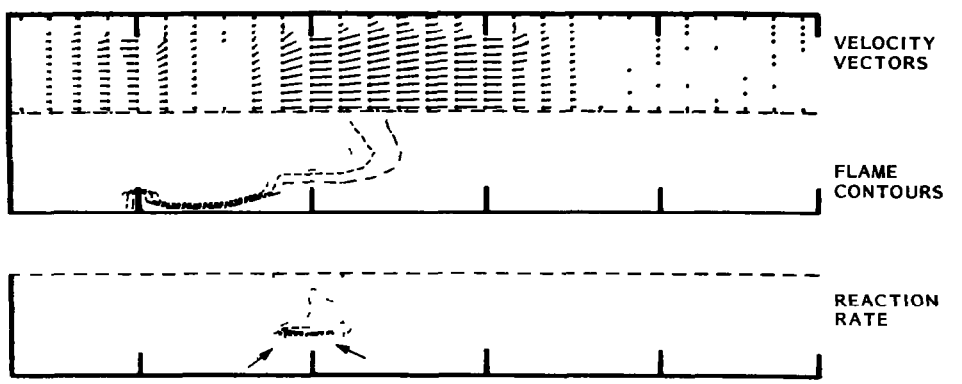

b METHANE/AIR

Fig 16 Distribution of velocity, flame and reaction rate for (a) propane—air and (b) methane—air explosions after the flame has passed the second obstacle Arrows indicate quenched region

flow is large Obviously, as seen in Fig 16, this quenching is most pronounced for the methane—air mixture, since the chemical induction time is much larger for methane than for propane The arrows in Fig 16b indicate the extinction region of the methane—air flame This difference in flame propagation between methane and propane continues also for the rest of the flame travel The net result of this is, as shown in Figs 9 and 10, that the pressures produced in methane—air explosions are lower by a factor of approximately 2 compared to propane—air explosions for identical geometries

Vented channel

As can be seen from the previous discussion, confinement on either side of the flame propagation path produces high flame speeds and pressures Chan et al [24] have performed a small scale study in which they investigated the influence of variable venting in a channel along the propagation path The layout of their channel is shown in Fig 17 The length of the channel was 1 22 m and the height was 0 203 m, with sharp-edged repeated obstacles which block off approximately 25% of the free channel area The experiments were performed using a homogeneous stoichiometric mixture of methane in air They found that the flame speed was drastically reduced by reducing the top confinement, as is shown in Fig 18a Bakke and Hjertager [25] used these data in a validation study of the model presented above Figure 18 shows a comparison between the measured and predicted variation of flame speed versus degree of confinement The figure shows that there is a close agreement between predictions and experiments Both the decrease in flame speed and the difference between obstacles along the wall and along the centre line are fairly well reproduced Also shown in Fig 18 is the influence of moving the obstacles off the wall and off the centre line Both of these cases show flame speeds in between the two extremes Figure

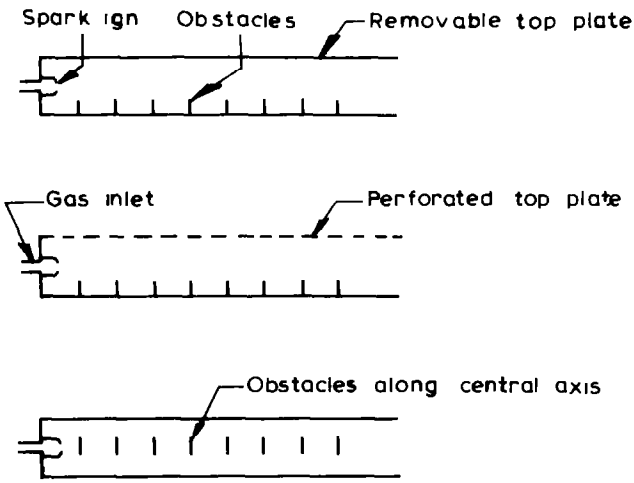

Fig 17 Schematics of experimental apparatus (Chan et al [24])

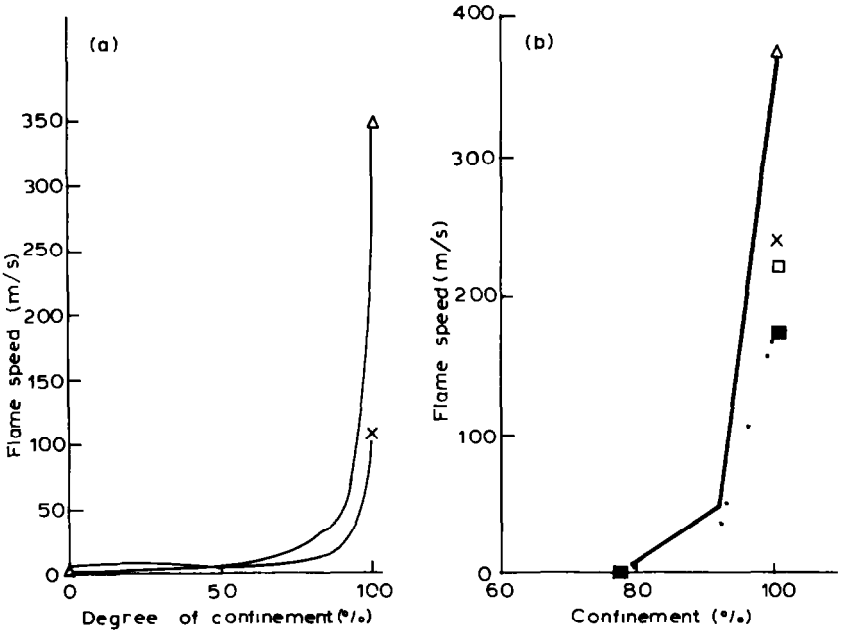

Fig 18 (a) Measured flame speeds vs confinement Measured 1 m from ignition △ — Obstacle at centre, × — obstacle at bottom (Chan et al [24]) (b) Predicted flame speed vs confinement Calculated 1 m from ignition △ — Obstacle in centre, × — obstacle off centre, □ — obstacle off wall, ■ — obstacle at wall (Bakke and Hjertager [25])

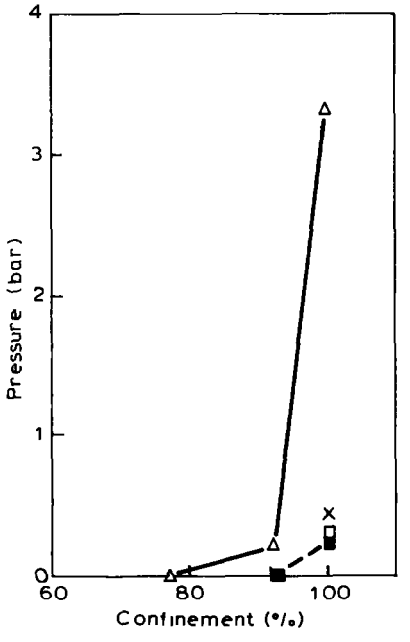

Fig 19 Pressure vs confinement, monitored near lid and open end, maximum value △ — Obstacle in centre, × — obstacle off centre, □ — obstacle off wall, ■ — obstacle at wall (Bakke and Hjertager [25])

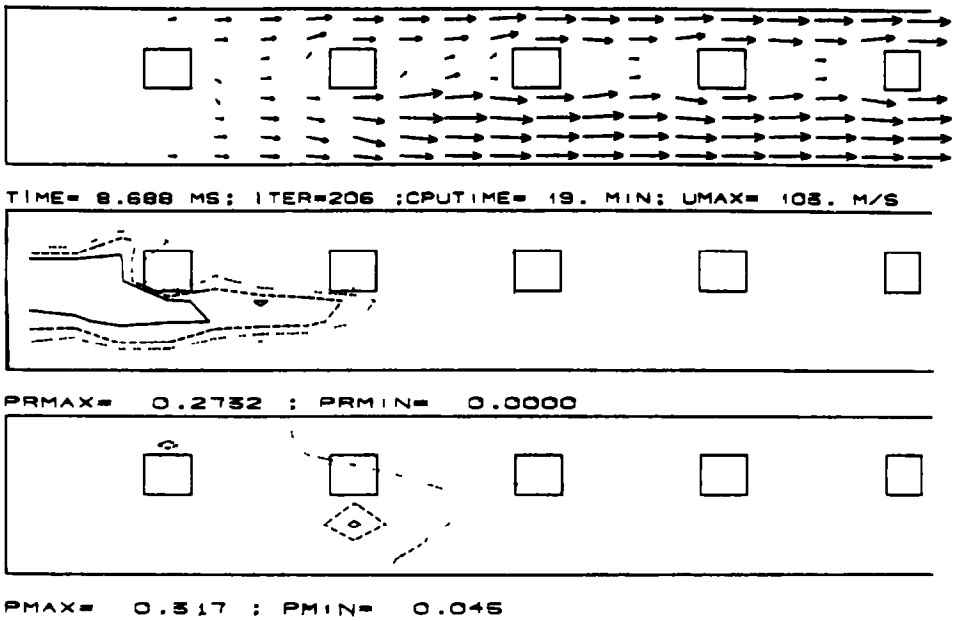

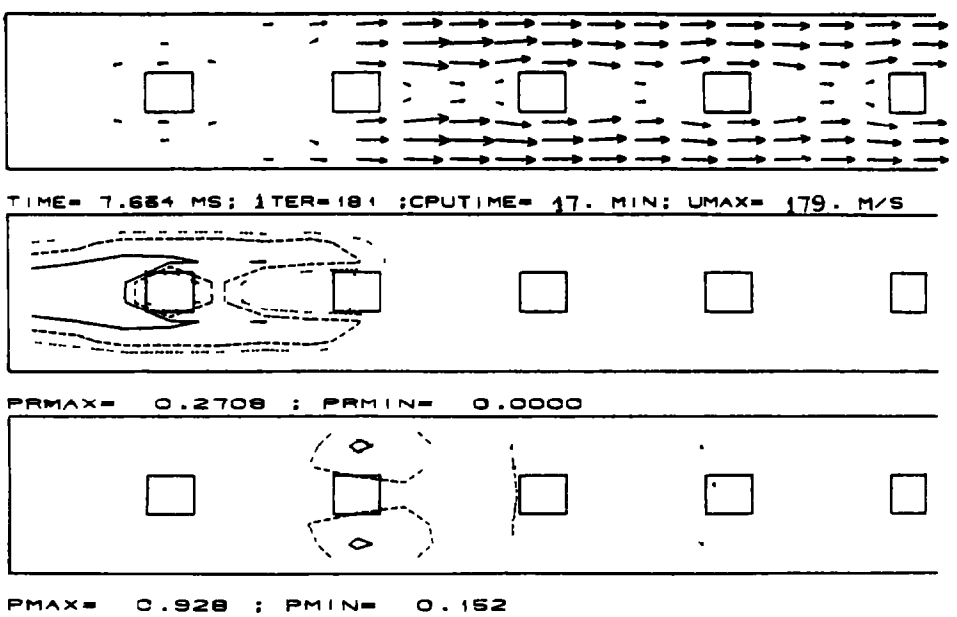

Fig 20 Distribution of velocity vectors, flame contours and pressure distribution for 100% confinement and two different obstacle arrangements (Bakke and Hjertager [25]) (top) Obstacles slightly off centre line, (bottom) obstacles along centre line

19 shows the predicted peak pressures versus confinement We observe that the maximum pressure of over 3 bar is obtained by placing the obstacles along the centre line, whereas moving the obstacles towards the wall reduced the pressures by a factor of 10 in this particular geometry. This shows that the maximum effectiveness of two shear layers is obtained only when the obstacles are exactly in the centreline Figure 20 shows the predicted distribution of flow velocities, flame contours and pressure contours for these two situations

4 7 Scaling characteristics

This last section will report on some predicted scaling characteristics of fuel—air explosions contained in tubes with a length over diameter ratio, L/D, of 4 0 and with 5 orifice rings (obstacles) which block off 30% of the free tube area, and in channels with L/D = 6 0 and 5 obstacles which block off 25% of the free channel area The obstacles are evenly distributed along the enclosure axis from the closed end to the open end, and ignition occurs at the closed end We take as our base case a tube with a length of 10 m and diameter of 2 5 m, and define a linear scaling factor of 1 0 for this geometry If, for example, we increase the length to 100 m and the diameter to 25 m, we have for this situation a linear scaling factor of 10 Explosion calculations have been performed over a range of scaling factors which cover three orders of magnitude, from 0 02 to 50 This corresponds to lengths of flame propagation from 20 cm to 500 m

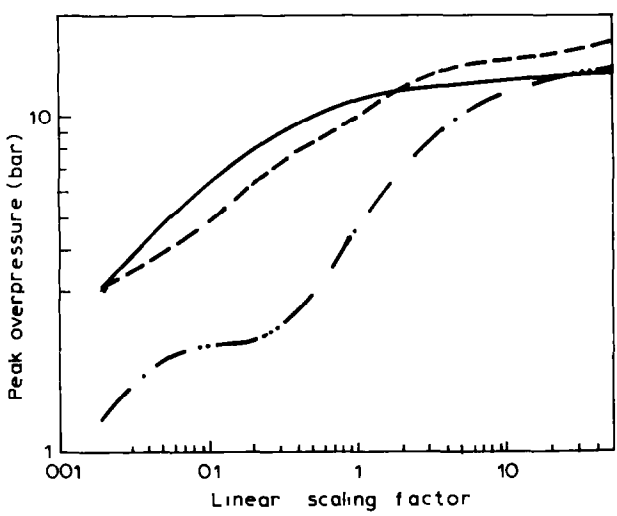

Fig 21 Variation of peak overpressure in stoichiometric mixtures of methane—air, propane—air and hydrogen—air with scaling Scaling factor of 1 0 indicates 10 m of flame travel over 5 obstacles L/D = 4, BR = 0 3, 5 obstacles —— = hydrogen, — — — = propane, — — = methane

For explosions contained in channels, we take a channel with length of 1 22 m and height of 0 203 m (Chan et al [24]) as the base, and define a length scale of 1 0 for this geometry If, for this case, we increase the length to 122 m and the height to 20 3 m we obtain a scaling factor of 100

Figure 21 shows the predicted peak overpressure produced in stoichiometric mixtures of methane—air, propane—air and hydrogen—air as a function of the linear scaling factor It can be seen that all three gases exhibit a strong dependence of peak pressure on scaling The larger the scale, the higher the explosion pressure Both hydrogen and propane produce larger pressures than methane It is observed that the difference in peak pressure ratio between propane and methane in a 0 5-m tube (linear scaling equals 0 05) is 2 0, a value which is in good accordance with the experimental results obtained by Bjørkhaug and Hjertager [14] in their 0 5-m radial geometry (see Fig 12 above)

Figure 22 shows the predicted peak overpressure produced by stoichiometric methane—air mixtures in a vented channel as function of length scale The figure shows that the effectiveness of venting is reduced with increasing scale For example, a vessel of length approximately 3 6 m (scale 3) and confinement fraction on top wall of 0 92 (8% porosity) will produce a pressure of 1 bar A scale-up of this geometry to a vessel with length of 25 m (scale 20) would produce a pressure of over 10 bar In order to reduce the pressure to below 1 bar a confinement fraction of the top wall smaller than 50% should be chosen (porosity larger than 50%) This indicates that larger scales needs larger vent areas to reduce the pressure to acceptable values

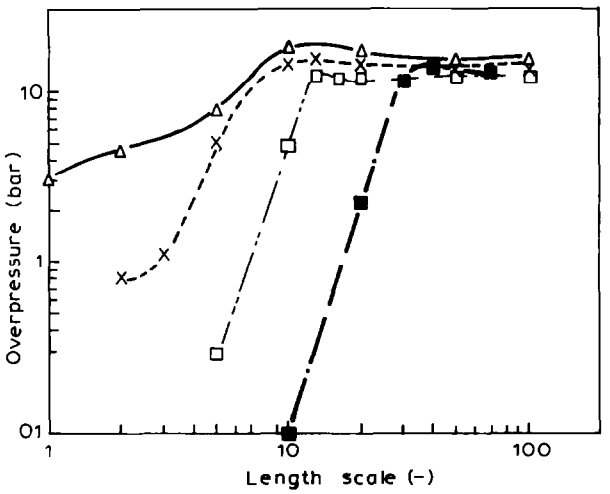

Fig 22 Maximum overpressure vs length scale Obstacles along central axis of channel ▫ — Confinement fraction 1 0, × — confinement fraction 0 92, ▫ — confinement fraction 0 77, ▪ confinement fraction 0 5 (Bakke and Hjertager [25])

5. Concluding remarks

(1) The venting area recommendations provided by some codes in current use may be totally inadequate for enclosures containing turbulence inducing obstacles
(2) To enable proper understanding of the complex processes which occur in turbulent gas explosions and enable reliable prediction of explosion pressures a thorough simulation model is presented This simulation model must, however, be further developed and validated against relevant data from both large- and small-scale experiments, prior to becoming a useful tool in safety assessment
(3) Further explosion pressure data from large-scale experiments in a variety of geometries are also badly needed to check the simulation model Thus the ability of the model to predict effects of high-density obstacle fields, radial and spherical modes of flame propagation and effects of real gas clouds is essential Experiments to elucidate some of these influences will be undertaken by the author and his colleagues

Acknowledgements

This work has been financially supported by BP Petroleum Development Ltd , Norway, Elf Aquitaine Norge A/S, Esso Exploration and Production Norway Inc , Mobil Exploration Norway Inc , Norsk Hydro and Statoil, Norway

References

1 W R Chapman and R V Wheeler, The propagation of flame in mixtures of methane and air Part IV The effect of restrictions in the path of the flame, J Chem Soc , (1926) 213, Part V The movement of the medium in which the flame travels, J Chem Soc , (1927) 38
2 K J Dorge, D Pangritz and H Gg Wagner, Experiments on velocity augmentation of spherical flames by grids, Acta Astron , 3 (1976) 1057—1076
3 I O Moen, M Donato, R Knystautas and J H S Lee, Flame acceleration due to turbulence produced by obstacles, Combust Flame, 39 (1980) 21—32
4 R K Eckhoff, K Fuhre, O Krest, C M Guirao and J H S Lee, Some recent large scale experiments in Norway, NTNF Project 18306500, Gas Explosions on Offshore Platforms, Flame Propagation and Pressure Development, Report CMI No 790750 1 Chr Michelsen Institute, Bergen, January 1980
5 I O Moen, J H S Lee, B H Hjertager, K Fuhre and R K Eckhoff, Pressure development due to turbulent flame propagation in large scale methane—air explosions, Combust Flame, 47 (1982) 31—52
6 B H Hjertager, K Fuhre, S J Parker and J R Bakke, Flame acceleration of propane—air in a large scale obstructed tube, 9th International Colloquium on Dynamics of Explosions and Reactive Systems, Poitiers, France, July 3—8, 1983
7 B H Hjertager, Simulation of transient compressible turbulent reactive flows, Com bust Sci Technol , 27 (1982) 159—170

8 B H Hjertager, Numerical simulation of turbulent flame and pressure development in gas explosions, Fuel—Air Explosions, SM Study No 16, University of Waterloo Press, Ontario, Canada, 1982, pp 407—426
9 H Matsui and J H S Lee, On the measure of the relative detonation hazards of gaseous fuel-oxygen and air mixtures, in Proc 17th Symposium (International) on Combustion, Combustion Institute, Pittsburgh, 1978, pp 1269—1289
10 D C Bull, Concentration limits to the initiation of unconfined detonation in fuel—air mixtures, Trans Inst Chem Eng , 57 (1979) 219—227
11 P Bradshaw, Turbulence, second corrected and updated edition, Springer Verlag, Berlin, 1978, p 144
12 B H Hjertager, K Fuhre and M Bjørkhaug, Effects of concentration on flame acceleration by obstacles in large-scale methane—air and propane—air explosions, Report CMI No 843403-5, Chr Michelsen Institute, Bergen, 1984
13 D Ballal and A H Lefebvre, The influence of flow parameters on minimum ignition energy and quenching distance, in Proc 15th Symposium (International) on Combustion, Combustion Institute, Pittsburgh, 1974, pp 1473—1481
14 M Bjørkhaug and B H Hjertager, The influence of obstacles on flame propagation and pressure development in a radial vessel, Report CMI No 823403-4, Chr Michelsen Institute, Bergen, 1982
15 C Chan, J H S Lee, I O Moen and P Thibault, Turbulent flame acceleration and pressure development in tubes, in Proc of the First Specialist Meeting (International) of the Combustion Institute, Universite de Bordeaux I, France, 1981, pp 479—484
16 C D Lind and J Whitson, Explosion hazards associated with spills of large quantities of hazardous materials, phase II, Department of Transportation, USCG Washington, DC, U S Coast Guard Report No CG-D-85-77, 1977
17 B E Launder and D B Spalding, The numerical computation of turbulent flows, Comput Meth Appl Mech Eng , (3) (1974) 269—289
18 B F Magnussen and B H Hjertager, On mathematical modelling of turbulent combustion with special emphasis on soot formation and combustion, in Proc 16th Symposium (International) on Combustion, Combustion Institute, Pittsburgh, 1976, pp 719—729
19 K Radhakrishnan, J B Heywood and R J Tabaczynski, Premixed turbulent flame blowoff velocity correlation based on coherent structures in turbulent flows, Combust Flame, 12 (1981) 19—33
20 B F Magnussen, On the structure of turbulence and a generalized eddy dissipation concept for chemical reaction in turbulent flow, in Proc 19th AIAA Aerospace Science Meeting, St Louis, Missouri, January 12—15, 1981
21 S V Patankar and D B Spalding, A calculation procedure for heat, mass and momentum transfer in three-dimensional parabolic flows, Int J Heat Mass Transfer, 15 (1972) 1787
22 A Burcat, R W Crossley and K Scheller, Shock tube investigation of ignition in ethane—oxygen—argon mixtures, Combust Flame, 18 (1972) 115—123
23 G L Schott and J L Kinsey, Kinetic studies of hydroxyl radicals in shock waves II Induction times in the hydrogen—oxygen reaction, J Chem Phys , 29 (1958) 1177—1182
24 C Chan, I O Moen and J H S Lee, Influence of confinement on flame acceleration due to repeated obstacles Combust Flame, 49 (1983) 27
25 J R Bakke and B H Hjertager, Numerical simulation of methane—air explosions in vented, obstructed channels Scaling characteristics, Report CMI No 823403-5, Chr Michelsen Institute, Bergen, 1983